Inverse Optimal Controller Design for a Quadrotor Unmanned Aerial Vehicle

Bora Bayraktaroğlu[1], Moayed Almobaied[2], Müjde Güzelkaya[3], İbrahim Eksin[4]

[1,2,3,4]Control and Automation Engineering Department, Istanbul Technical University, 34469 Maslak Istanbul, Turkey
{bayraktaroglubo, almobaied, guzelkaya, eksin}@itu.edu.tr

Abstract

This paper presents the application of inverse optimal control approach to an unmanned quadrotor air vehicle system. Here, the inverse optimal controller is designed to solve the reference tracking problem relying on the use of control Lyapunov function. In the establishment of the control law, the affine-in-input discrete-time nonlinear system model is taken into consideration. A stabilizing feedback control law is constructed such that control Lyapunov function is known a priori. After stability examination and determination of a meaningful cost functional, respective cost functional is optimized. Then, a matrix that minimizes a tracking error function is searched using PSO algorithm. The designed controller has been applied to a nonlinear model of a quadrotor. It is shown that the proposed controller guarantees a fast convergence and makes the quadrotor stabilize itself very fast and follow aggressive trajectories accurately under certain circumstances.

1. Introduction

In the last decade, due to a significant amount of effort on the development in key technologies of propulsion, flight control, communications, and sensors, a concentrated research effort has been conducted on designing and controlling quadrotor Unmanned Aerial Vehicles (UAVs) [1]. Nevertheless, UAVs are dynamically unstable systems that requires active control to stabilize the vehicle's attitude [2]. The classical control algorithms fail to perform aggressive manoeuvres of a quadrotor whose well-known characteristics are underactuated, highly nonlinear and strongly coupled with inextricably intertwined nature of the system dynamics [3, 4]. The control strategies presented for quadrotors include: PID, Linear Quadratic Regulator (LQR), Sliding mode, Backstepping, Feedback linearization, Adaptive, Robust, Optimal, L_1, H_∞, Fuzzy logic and Artificial neutral networks [5-11].

In the infinite horizon nonlinear optimal control problem, the aim is to find the control law to minimize a cost functional. The problem requires the solution of Hamilton Jacobi Bellman (HJB) equation which is extremely difficult and an analytical solution does not exist for general nonlinear systems [9]. Inverse Optimal Control (IOC) theory views the problem from a different perspective, namely, construct a stabilizing feedback control law for a given plant at first, then find a meaningful cost functional that depends on the state variables and control inputs for which the stabilizing controller is optimal [12, 13]. There are only few studies focused on IOC of quadrotors. Authors in [12] employed inverse optimal control strategy for a discrete time nonlinear system based on the approach given in [14]**.** Likewise, both in [15] and [16] the same inverse optimal control strategy is used to test the effectiveness of the inverse optimal control theory for trajectory tracking purposes.

In this paper, the control of quadrotor UAV is proposed using IOC approach based on the definition of a Control Lyapunov Function (CLF) [17]. In this IOC approach the control law is established using a CLF and the inverse optimal problem transforms to the determination of an appropriate scalar matrix [12, 13]. Firstly, nonlinear model of UAV is obtained in discrete time nonlinear affine in input system equations. Then, a multi-objective particle swarm optimization (MOPSO) algorithm is proposed to optimize the parameters of IOC in an off-line manner. The developed control strategy minimizes a cost functional while accomplishing the task of improving quadrotor stability and trajectory tracking.

This paper is organized in five chapters as follows: chapter 2 describes nonlinear dynamical model for the quadrotor system. Inverse optimal control method is covered in chapter 3. Chapter 4 contains trajectory tracking performance analysis based on simulation results. Finally, chapter 5 covers achievements of this research.

2. Modelling of Quadrotor UAV

In chosen ("+") configuration, *X* axis lies along the arm of motor arm, *Y* axis lies along the motor arm 2, and the Z axis is the vertical axis pointing upwards where d is the distance from the motor to the axis of rotation [18]. This research focuses on the control of row angle, pitch angle, yaw angle and altitude of the quadrotor. The assumptions listed below,

- The structure is supposed rigid and symmetrical.
- The center of gravity and the body fixed frame origin are assumed to coincide.
- Earth fixed frame is assumed to be inertial.
- The propellers are supposed rigid.
- Thrust and drag are proportional to the square of propeller's rotational speed.

2.1. Nonlinear Model of UAV

The equations of motion are given as follows [19]:

$$\ddot{\phi} = \dot{\theta}\dot{\psi}\left(\frac{1}{J_{xx}}\left(J_{yy} - J_{zz}\right)\right) + \dot{\theta}\frac{J_r}{J_{xx}}\Omega_r + \frac{1}{J_{xx}}u_2. \quad (1)$$

$$\ddot{\theta} = \dot{\phi}\dot{\psi}\left(\frac{1}{J_{yy}}\left(J_{zz} - J_{xx}\right)\right) - \dot{\phi}\frac{J_r}{J_{yy}}\Omega_r + \frac{1}{J_{yy}}u_3. \quad (2)$$

$$\ddot{\psi} = \dot{\theta}\dot{\phi}\left(\frac{1}{J_{zz}}\left(J_{xx} - J_{yy}\right)\right) + \frac{1}{J_{zz}}u_4. \quad (3)$$

$$\ddot{z} = g - (cos\phi cos\theta)\frac{1}{m}u_1. \quad (4)$$

$$\ddot{x} = (cos\phi sin\theta cos\psi + sin\phi sin\psi)\frac{1}{m}u_1 \ . \quad (5)$$

$$\ddot{y} = (cos\phi sin\theta sin\psi - sin\phi cos\psi)\frac{1}{m}u_1 \ . \quad (6)$$

Body-fixed frame and earth-fixed frame are represented by $(C, \overrightarrow{b_1}, \overrightarrow{b_2}, \overrightarrow{b_3})$ and $(O, \overrightarrow{e_1}, \overrightarrow{e_2}, \overrightarrow{e_3})$ respectively [18].

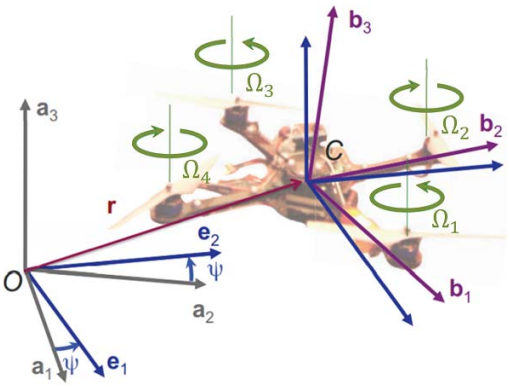

Fig. 1. The position and orientation of the vehicle with respect to the world.

Four rotational velocities of the motors are represented by $\Omega_1,\ \Omega_2, \Omega_3, \Omega_4$ as illustrated in Fig.1. The input vector is given as [20],

$$u = [u_1\ \ u_2\ \ u_3\ \ u_4]^T \tag{7}$$

$$u_1 = b(\Omega_1{}^2 + \Omega_2{}^2 + \Omega_3{}^2 + \Omega_4{}^2) \tag{8}$$

$$u_2 = b(-\Omega_2{}^2 + \Omega_4{}^2) \tag{9}$$

$$u_3 = b(\Omega_1{}^2 - \Omega_3{}^2) \tag{10}$$

$$u_4 = d(-\Omega_1{}^2 + \Omega_2{}^2 - \Omega_3{}^2 + \Omega_4{}^2) \tag{11}$$

The state vector is chosen as,

$$X = [x_1\ \ x_2\ \ x_3\ \ x_4\ \ x_5\ \ x_6\ \ x_7\ \ x_8\ \ x_9\ \ x_{10}\ \ x_{11}\ \ x_{12}]^T = \\ = [x\ \ y\ \ z\ \ \dot{x}\ \ \dot{y}\ \ \dot{z}\ \ \phi\ \ \theta\ \ \psi\ \ \dot{\phi}\ \ \dot{\theta}\ \ \dot{\psi}]^T \tag{12}$$

In this model, the state variables x_1, x_3, x_5 represent roll, pitch, yaw angles; x_2, x_4, x_6 represent roll, pitch, yaw angle rates; x_9, x_{11}, x_7 represent positions along x, y, z axes; x_{10}, x_{12}, x_8 represent velocities along x, y, z axes. The total thrust is (u_1) $[N]$. u_2, u_3, u_4 $[Nm]$ represent roll, pitch and yaw torques, respectively. b is thrust coefficient, d is drag coefficient, m is the total mass of quadrotor, g is the acceleration due to gravity, Ω_r is gyroscopic forces produced by motor and the moment of inertia of quadrotor about X, Y and Z axes are denoted by J_{xx}, J_{yy} and J_{zz}, respectively.

2.2. Affine-in-input Discrete Time Model

The IOC method requires discrete-time affine-in-input nonlinear state equations. In order to discretize the equations in Section 2.1, we use Euler approximation given below:

$$\dot{x}_i = \frac{x_{i,(k+1)} - x_{i,k}}{\Delta T} \tag{13}$$

Here, ΔT is the sampling time. The affine in the input nonlinear state equations are described in the following form:

$$x_{k+1} = f(x_k) + g(x_k)u_k \tag{14}$$

where $x \in \mathbb{R}^n$ is the state of the system; $u \in \mathbb{R}^m$ is the control input; $f(x_k): \mathbb{R}^n \to \mathbb{R}^n$ and $g(x_k): \mathbb{R}^n \to \mathbb{R}^{n*m}$ are smooth matrices. Using the nonlinear model in Section 2.1, we obtain the expressions for $f(x_k)$ and $g(x_k)$ in (14) as follows:

$$f(x_k) = \begin{pmatrix} x_{1,k} + \Delta T(x_{2,k}) \\ x_{2,k} + \Delta T(\frac{1}{J_{xx}}(J_{yy} - J_{zz})x_{4,k}x_{6,k}) \\ x_{3,k} + \Delta T(x_{4,k}) \\ x_{4,k} + \Delta T(\frac{1}{J_{yy}}(J_{zz} - J_{xx})x_{2,k}x_{6,k}) \\ x_{5,k} + \Delta T(x_{6,k}) \\ x_{6,k} + \Delta T(\frac{1}{J_{zz}}(J_{xx} - J_{yy})x_{2,k}x_{6,k}) \\ x_{7,k} + \Delta T(x_{8,k}) \\ x_{8,k} + \Delta T(g) \\ x_{9,k} + \Delta T(x_{10,k}) \\ x_{10,k} \\ x_{11,k} + \Delta T(x_{12,k}) \\ x_{12,k} \end{pmatrix} \tag{15}$$

$$g(x_k) = \begin{pmatrix} 0 & 0 & 0 & 0 \\ 0 & \frac{1}{J_{xx}} & 0 & 0 \\ 0 & 0 & 0 & 0 \\ 0 & 0 & \frac{1}{J_{yy}} & 0 \\ 0 & 0 & 0 & 0 \\ 0 & 0 & 0 & \frac{1}{J_{zz}} \\ 0 & 0 & 0 & 0 \\ -\Delta T(cosx_{1,k}cosx_{3,k})\frac{1}{m} & 0 & 0 & 0 \\ 0 & 0 & 0 & 0 \\ \Delta T(cosx_{1,k}sinx_{3,k}cosx_{5,k} + sinx_{1,k}sinx_{5,k})\frac{1}{m} & 0 & 0 & 0 \\ 0 & 0 & 0 & 0 \\ \Delta T(cosx_{1,k}sinx_{3,k}sinx_{5,k} - sinx_{1,k}cosx_{5,k})\frac{1}{m} & 0 & 0 & 0 \end{pmatrix} \tag{16}$$

3. Inverse Optimal Controller Design

Consider the affine-in-input nonlinear state equations expressed in the form (14). The infinite horizon nonlinear optimal control problem is to find the control law u_k such that the following cost functional is minimized:

$$V(x_k) = \sum_{n=k}^{\infty}(L(x_n) + u_n^T R u_n) \tag{17}$$

where

V: $\mathbb{R}^n \to \mathbb{R}^+$ is the cost functional;

L: $\mathbb{R}^n \to \mathbb{R}^+$ is positive semi-definite function;

$R: \mathbb{R}^n \to \mathbb{R}^{n*m}$ is a real symmetric positive definite weighting matrix which could be a function of states of the system [12].

The boundary condition of the cost functional is assumed to be zero (i.e., $V(x = 0) = 0$). The optimal control u_k^* is obtained by applying Bellman's principle of optimality in the form as shown below:

$$u_k^* = -\frac{1}{2}R^{-1}g^T(x_k)\frac{\partial V^*(x_{k+1})}{\partial x_{k+1}} \tag{18}$$

where $\frac{\partial V^*(x_{k+1})}{\partial x_{k+1}}$ can be derived from the analytical solution of the following discrete-time HJB equation:

$$V^*(x_k) = L(x_k) + V^*(x_{k+1}) + \\ \frac{1}{4}\frac{\partial V^{*T}(x_{k+1})}{\partial x_{k+1}}g(x_k)R^{-1}g^T(x_k)\frac{\partial V^*(x_{k+1})}{\partial x_{k+1}} \tag{19}$$

Analytical solution of HJB equation is usually very difficult for a general nonlinear system. In this regard, IOC have

yielded encouraging results for a variety of real world applications. In [21], a control law is associated with a (CLF).

Definition 3.1. The control law u_k^* in (19) is inverse optimal control if
(i) it achieves (global) exponential stability of the equilibrium point $x_k = 0$ for the system in (14).
(ii) it minimizes the cost functional in (17). For which $L(x_k) = -\bar{M}$, and $M(x_k)$ is radially unbounded positive definite function such that inequality,

$$\bar{M} := M(x_{k+1}) - M(x_k) + u_k^{*T} R u_k^* \leq 0 \tag{20}$$

is fulfilled [21].

Thus, a CLF $M(x_k)$ is proposed such that (i) and (ii) in Definition 3.1 are guaranteed [12]. A candidate quadratic control Lyapunov function $M(x_k)$ can be proposed in the following form:

$$M(x_k) = \frac{1}{2} x_k^T P x_k \tag{21}$$

where $P \in \mathbb{R}^{n*n}$ is assumed to be positive definite $P > 0$ and symmetrical $P = P^T$ matrix. The state feedback control law, described by (19) can then be rewritten as:

$$u_k^* = -\frac{1}{2}\left(R + \frac{1}{2} g^T(x_k) P g(x_k)\right)^{-1} * g^T(x_k) P f(x_k) \tag{22}$$

A necessary condition for matrix P to satisfy the requirements of Definition 3.1 is given by Theorem 3.1 [14] as follows:

Theorem 3.1. Consider the system in (17). If there exists a matrix $P = P^T > 0$ such that the following inequality holds:

$$M_f(x_k) - \frac{1}{4} P_1^T(x_k)(R + P_2(x_k))^{-1} * P_1(x_k) \leq -\zeta_Q \|x_k\|^2 \tag{23}$$

where $M_f(x_k) = M(f(x_k)) - M(x_k)$, with $M(f(x_k)) = \frac{1}{2} f^T(x_k) P f(x_k)$; $\zeta_Q > 0$; $P_1(x_k) = g^T(x_k) P\, f(x_k)$; $P_2(x_k) = \frac{1}{2} g^T(x_k) P\, g(x_k)$; then, the global exponential stabilization of the equilibrium point $(x_k = 0)$ of the system is achieved by the control law (23). The selection of an appropriate P matrix is an active research topic [12, 15, 16].

To transform the regulator based above IOC formulation to trajectory tracking as in [16], the tracking error vector can be described as follows:

$$\tilde{x}_k = x_k - r_k \tag{24}$$

where $r_k \in \mathbb{R}^n$ is the reference vector with the same dimension as the state vector. By evaluating (24) at time $(k + 1)$, tracking error dynamics is given by

$$\tilde{x}_{k+1} = x_{k+1} - r_{k+1} \tag{25}$$

To derive the dynamics of the new system, the value of x_{k+1} is put into (25) so that the following formula is obtained

$$\tilde{x}_{k+1} = f(x_k) + g(x_k) u_k - r_{k+1} \tag{26}$$

which can be arranged into a new affine discrete time nonlinear system with new system dynamics

$$\tilde{x}_{k+1} = \tilde{f}(\tilde{x}_k) + g(x_k) u_k \tag{27}$$

where

$$\tilde{f}(\tilde{x}_k) = f(x_k) - r_{k+1} \tag{28}$$

The reference signal is delayed one step to ensure the causality of the control implementation. As a result, the following stabilizing control law equation is obtained as:

$$u_k^* = -\frac{1}{2}\left(R + \frac{1}{2} g^T(x_k) P g(x_k)\right)^{-1} * g^T(x_k) P \tilde{f}(\tilde{x}_k) \tag{29}$$

where R and P are positive semi-definite matrices. Given the reference vector $r_d(t)$, the controller, actuator and quadrotor system together can be represented as in Figure 2 [22].

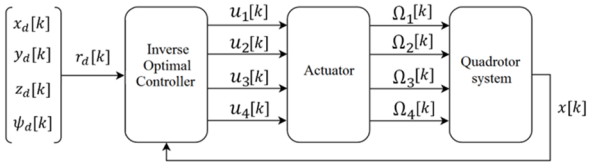

Fig. 2. Control scheme of the proposed inverse optimal controller.

4. Inverse optimal controller design for quadrotor UAV based on multi objective PSO algorithm

In this study the PSO algorithm is used to optimize P and R matrices given in Section 3. The dimension of P matrix given in (21) is *12x12* for the UAV problem. Since searching for all elements of P matrix is infeasible, we try to find out a special sparse structure of the matrix P by heuristic reasoning on trial and error experiments.

For positive definiteness condition Cholesky decomposition is employed and PSO algorithm is first used to find the elements of a lower triangular matrix P_1 ($P = P_1 {P_1}^T$).

An objective function is evaluated along the chosen representative path to be tracked. The trajectory tracking fitness is defined as follows:

$$f = \sum_{k=1}^{s} \sqrt{\frac{w_1(X_1[k] - X_{1ref}[k])^2 + w_2(X_2[k] - X_{2ref}[k])^2 + .. + w_n(X_n[k] - X_{nref}[k])^2}{n}} \tag{30}$$

The roll angle is constrained with a limit (ϕ_{i_max}). If the roll angle goes above this value, an error term is added to the tracking error function. However, the error is set to zero whenever the roll angle is below the limit.

$$\phi_{i\_excess} = \begin{cases} |\phi_i - \phi_{i_{\mathrm{m}}}| & |\phi_i| \geq \phi_{i\_max} \\ 0 & |\phi_i| < \phi_{i\_max} \end{cases} \tag{31}$$

The same logic is applied to the pitch angle which is also constrained with a limit (θ_{i_max}) similarly to roll angle

$$\theta_{i\_excess} = \begin{cases} |\theta_i - \theta_{i\_max}| & |\theta_i| \geq \theta_{i\_max} \\ 0 & |\theta_i| < \theta_{i\_max} \end{cases} \tag{32}$$

The following excess attitude term is added to the tracking error function value

$$f_{att} = c * \sum_{k=1}^{s} \sqrt{(\phi[k]_{i\_excess})^2 + (\theta[k]_{i\_excess})^2} \tag{33}$$

R matrix in (29) plays the vital role in the control signal. In the optimization procedure the off-diagonal elements of matrix R are taken to be zero. Moreover, the values of the second (roll command) and third (pitch command) diagonal elements are assumed to be equal. Therefore, only 3 diagonal elements of the matrix are needed to be optimized.

The optimization process basically consists of five steps:

Step 1. Configure PSO to optimize a P_1 matrix.

Step 2. For every member of the swarm the objective function is evaluated as follows:

Step 3.1. Form the P matrix from the swarm members

Step 3.2. Obtain the positive definite P_1 matrix using ($P = P_1 {P_1}^T$).

Step 3.3. Form the matrix R from the swarm members (if needed).

Step 3.4. Simulate the system under IOC tracking control for a time T. For every discrete time step do the following:

Step 3.4.1. Calculate system matrices $f(x_k), \tilde{f}(\tilde{x}_k), g(x_k)$.

Step 3.4.2. Calculate the IOC feedback signal u_k using the obtained P and R matrices.

Step 3.4.3. Clip the control signal u_k (if needed).

Step 3.4.4. Evaluate the basic fitness function along the trajectory.

Step 3.4.5. Add the attitude penalty term (if needed).

Step 3.5. Return the accumulated fitness value to PSO algorithm.

Step 4. Run PSO for changes in the effective elements of P_1 and R matrices.

Step 5. Go back to step 2 unless the termination criteria is met.

5. Simulation Results

Initial conditions for the tracking problem of UAV system are chosen as:

$x_{10} = 0.5,\ x_{20} = 0.5,\ x_{30} = 0.8,\ x_{40} = 0.1,\ x_{50} = 0.08,\ x_{60} = -4.2,\ x_{70} = -0.1,\ x_{80} = -0.15,\ x_{90} = 0.25,\ x_{100} = 0.1,\ x_{110} = 0.1$ and $x_{120} = 0.3$.

The quadrotor parameters are given in Table 1. Also, the parameters of PSO are chosen default as shown in Table 2 based on MATLAB PSO Research Toolbox [22]. The number of recursions is chosen as 2500 where the sampling period is set as 0.01s.

A full lower triangle matrix of P_1 matrix consists 78 parameters; however, it is not possible to get a reasonable result with such a large population size in PSO algorithm. It is observed that the specialized 28 elements have vital role on the system. Thus, a special structure of P_1 with 28 (12 diagonal elements and 16 off-diagonal elements) non-zero elements is found by trial and error. Moreover, the maximum value for these non-zero elements is selected as 500.

Table 1. UAV parameters

Parameter	Description	Value/Unit
m	Gross weight	1.023 kg
J_{xx}	Moment of inertia around x-axis	0.096 kgm^2
J_{yy}	Moment of inertia around y-axis	0.096 kgm^2
J_{zz}	Moment of inertia around z-axis	0.018 kgm^2
b	Thrust coefficient	1.59 x10^{-7} N/rpm^2
d	Drag coefficient	3 x10^{-9} Nm/rpm^2
g	Acceleration due to gravity	9.81 m/s^2

Table 2. PSO parameters

Parameter	Description	Value
χ	Constriction factor	1.4142
c_1	Cognitive learning rate	1.4962
c_2	Social learning rate	1.4962

where $\chi = \frac{2}{\left|2-\varphi-\sqrt{\varphi^2-4\varphi}\right|}$ and $\varphi = c_1 + c_2$.

The chosen R matrix is R= diag(0.01, 0.01, 0.01, 0.01) and the optimized P matrix is obtained as:

P=

$$\begin{bmatrix}
9.03x10^3 & 1.4173 & 0 & 0 & 0 & 0 & 0 & 0 & 0 & 0 & 0 & 0 \\
1.4173 & 57.377 & 0 & 0 & 1.36x10^3 & 0.2779 & 0 & 0 & 0 & 0 & 1.59x10^3 & 38.0407 \\
0 & 0 & 4.52x10^5 & 0 & 0 & 0 & 0 & 0 & 0 & 0 & 0 & 0 \\
0 & 0 & 0 & 1.63x10^{-5} & 0.2834 & 2.04x10^{-4} & 0 & 0 & 1.9988 & 0.047 & 0 & 0 \\
0 & 1.36x10^3 & 0 & 0.2834 & 9.19x10^5 & 2.83x10^3 & 0 & 0 & 5.02x10^4 & 816.2378 & 2.98x10^5 & 5.1x10^3 \\
0 & 0.2779 & 0 & 2.04x10^3 & 2.83x10^3 & 15.2982 & 0 & 0 & 78.5619 & 0.5898 & 187.1366 & 1.0399 \\
0 & 0 & 0 & 0 & 0 & 0 & 2.5x10^5 & 1.08x10^4 & 0 & 0 & 0 & 0 \\
0 & 0 & 0 & 0 & 0 & 0 & 1.08x10^4 & 474.8032 & 0 & 0 & 0 & 0 \\
0 & 0 & 0 & 1.9988 & 5.02x10^4 & 78.5619 & 0 & 0 & 2.45x10^5 & 5.75x10^3 & 0 & 0 \\
0 & 0 & 0 & 0.047 & 816.2378 & 0.5898 & 0 & 0 & 5.75x10^3 & 135.3159 & 0 & 0 \\
0 & 1.59x10^3 & 0 & 0 & 2.98x10^5 & 187.1366 & 0 & 0 & 0 & 0 & 2.77x10^5 & 5.95x10^3 \\
0 & 38.0407 & 0 & 0 & 5.1x10^3 & 1.0399 & 0 & 0 & 0 & 0 & 5.95x10^3 & 142.3332
\end{bmatrix}$$

(12x12)

Simulation results of the system are shown in Figure 3 and 4 where k is the discrete time index. Tracking errors are given in Table 3.

Table 3. RMS errors of tracking

Parameter	Description	Value/Unit
$RMS\ (e_x)$	RMS error of x position	0.0073 m
$RMS\ (e_y)$	RMS error of y position	0.008 m
$RMS\ (e_z)$	RMS error of z position	0.0098 m
$RMS\ (e_\psi)$	RMS error of ψ angle	0.0032 rad

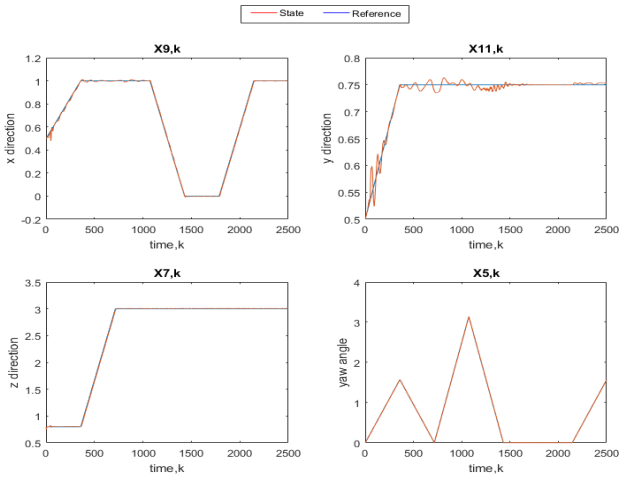

Fig. 3. Response of the state variables x_9, x_{11}, x_7 (positions along x, y, z axes), x_5 (yaw angle).

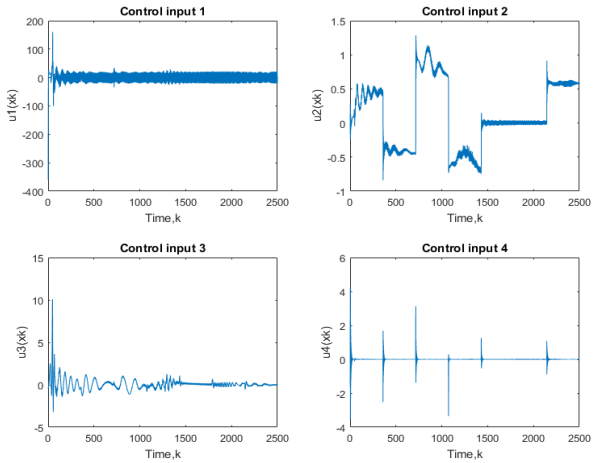

Fig. 4. Control input responses.

6. Conclusion

In this paper, the control of quadrotor UAV is proposed using IOC approach based on CLF. Firstly, nonlinear model of UAV is obtained in discrete time nonlinear affine-in-input system equations. Then, a multi-objective particle swarm optimization algorithm guaranteeing stability is proposed to optimize the parameters of IOC in an off-line manner. The developed control strategy minimizes a cost functional while accomplishing the task of improving quadrotor stability and trajectory tracking. The designed controller has been applied to a nonlinear model of a quadrotor. The proposed controller makes the quadrotor stabilize itself very fast and follow aggressive trajectories accurately under certain circumstances.

7. References

[1] Davis, W. R., Jr., Kosicki, B. B., Boroson, D. M., and Kostishack, D. F. (1996). "Micro Air Vehicles for Optical Surveillance," The Lincoln Laboratory Journal, 9(2), pp. 1-2.

[2] Miller, D. S. (2011). Open loop system identification of a micro quadrotor helicopter from closed loop data (Master's thesis, University of Maryland, USA).

[3] Özbek, N. S., Önkol, M., Efe, M. Ö. (2016). "Feedback Control Strategies for Quadrotor Type Aerial Robots- A Survey," Transactions of the Institute of Measurement and Control, 38(5), pp. 529-554.

[4] He, Z. F., and Zhao, L. (2014). "A Simple Attitude Control of Quadrotor Helicopter Based on Ziegler-Nichols Rules for Tuning PD Parameters," Scientific World Journal, pp. 13.

[5] Fowers, S. (2008). Stabilization and Control of a Quad-rotor Micro-UAV Using Vision Sensors (Master's thesis, Brigham Young University, Utah, USA).

[6] Singh, P. (2015). Development of Unmanned Aerial Vehicle (Quadcopter) with Real-time Object Tracking (Master of Technology, National Institute of Technology, Orissa, India).

[7] Tayebi, A., and McGilvray, S. (2004). "Attitude stabilization of a four-rotor aerial robot," In: *IEEE Conf. on Decision and Control*, vol. 2, pp. 1216-1221.

[8] Zemalache, K., Beji, L., and Marref, H. (2005). "Control of an under-actuated system: application a four rotors rotorcraft," In: *IEEE Int. Conf. on Robotics and Biomimetics (ROBIO)*, pp. 404-409.

[9] Mokhtari A., and Benallegue, A. (2004). "Dynamic feedback controller of Euler angles and wind parameters estimation for a quadrotor unmanned aerial vehicle,"In: *IEEE International Conference on Robotics and Automation (ICRA)*, vol. 3, 2004, pp. 2359–2366.

[10] Voos, H. (2006). "Nonlinear state-dependent Riccati equation control of a quadrotor UAV," In: *IEEE Conf. on Computer Aided Control System Design*, IEEE Int. Conf. on Control Applications, IEEE Int. Symposium on Intelligent Control, Munich, Germany, pp. 2547-2552.

[11] Jang J. S., Waslander, S. L., Hoffmann G. M., and Tomlin, C. T. (2005). "Multi-Agent Quadrotor Testbed Control Design: Integral Sliding Mode vs. Reinforcement Learning" In: *IEEE/RSJ International Conf. on Intelligent Robots and Systems*, AB, CA, pp. 468-473.

[12] Almobaied, M., Eksin, I., Güzelkaya, M. (2017). "Inverse Optimal Controller Design Based on Multi-Objective Optimization Criteria for Discrete-Time Nonlinear Systems," *Optimal Control Applications and Methods*.

[13] Margaliot, M. And Langholz, G. (2001). Some nonlinear optimal control problems with closed-form solutions. Int. Journal on Robust Nonlinear Control, 11(14), 1365-1374.

[14] Ornelas, F., Sanchez, E. N. and Loukianov, A. G. (2011). "Discrete-time nonlinear systems inverse optimal control: A control Lyapunov function approach," In: *IEEE Int. Conf. on Control Applications*, pp. 1431–1436.

[15] Ornelas, F., Sanchez, E. N., and Loukianov, A. G. (2010). "Discrete-time inverse optimal control for nonlinear systems trajectory tracking," In: *IEEE Conf. on Decision and Control*, Atlanta, USA, pp. 4813-4818.

[16] Ruiz-Cruz, R., Sanchez, E. N., Ornelas-Tellez, F., and Loukianov, A. G. (2012). "Particle Swarm Optimization for Discrete-time Inverse Optimal Control of a Doubly Fed Induction Generator," In: *IEEE Transactions on Cybernetics*, 2012, (43)6, pp. 1698-1709.

[17] Almobaied, M., Eksin, I., Güzelkaya, M. (2015). "A new inverse optimal control method for discrete-time systems," In: *12th Int. Conf. on Informatics in Control, Automation and Robotics (ICINCO)*, vol.01, pp.275-280.

[18] Kumar, V., and Michael, N. (2012). Opportunities and challenges with autonomous micro aerial vehicles. Int. Journal of Robotics Research, 31(11), pp. 1279-1291.

[19] Bouabdallah, S. (2004). "Design and control of an indoor micro quadrotor," In: *Int. Conf. on Robotics and Automation*, vol. 5, pp. 4393-4398.

[20] Voos, H., and Bou-Ammar, H. (2010). "Nonlinear tracking and landing controller for quadrotor aerial robots". In: *IEEE Int. Conf. on Control Applications (CCA)*, Yokohama, pp. 2136-2141.

[21] Sanchez, E. N., and Ornelas-Tellez, F. (2013). "Discrete-Time Inverse Optimal Control for Nonlinear Systems," *CRC Press*.

[22] Bayraktaroglu, B. (2017). Tracking Control Methodologies for a Quadrotor UAV (Master's thesis, Istanbul Technical University, Istanbul, Turkey).